Journal of Applied Fluid Mechanics, Vol. 18, No. 5, pp. 1217-1230, 2025.
Available online at www.jafmonline.net, ISSN 1735-3572, EISSN 1735-3645.
https://doi.org/10.47176/jafm.18.5.3054

Enhanced Numerical Simulation Study of Accelerated Demulsification in Dilute Emulsions under Pulsed Electric Field Control

Y. Wu, H. Wang and X. Zhang †

Key Laboratory of Engineering Mathematics and Advanced Computing of Nanchang Institute of Technology, School of Sciences, Nanchang Institute of Technology, Nanchang 330099, People's Republic of China

†*Corresponding Author Email: zhangxh@nit.edu.cn*

ABSTRACT

This study simulates the dynamic evolution of demulsification in emulsions under various electric field parameters, using a multicomponent lattice Boltzmann color model that integrates pulsed electric and flow fields. The degree of aggregation of dispersed-phase droplets is quantitatively analyzed using the area-to-circumference ratio. Results of numerical simulation demonstrate the demulsification behavior of dilute emulsions under three types of pulsed electric fields: direct current (DC) pulsed electric field, unidirectional triangular pulsed electric field, and bidirectional triangular pulsed electric field. Findings indicate the occurrence of electrophoretic and oscillatory coalescence in dilute emulsions under pulsed electric fields. The improved bidirectional triangular pulsed electric field shows enhanced efficiency relative to that of either the DC pulsed or the unidirectional triangular pulsed electric field. Moreover, the enhanced bidirectional triangular pulsed electric field effectively demulsifies oil-in-water dilute emulsions and prevents oil droplets disintegration under high-voltage across different component ratios.

Article History

Received September 2, 2024
Revised November 13, 2024
Accepted December 14, 2024
Available online March 4, 2025

Keywords:

Lattice Boltzmann
Color model
Pulsed electric field
Demulsification

1. INTRODUCTION

Oily wastewater has increasingly contributed to severe pollution as global industrialization advances. Its biodegradation presents a challenge, owing to its composition and significant threat to the environment. Thus, it has drawn interest in environmental protection (Yang, 2007; Zhang et al., 2022). Stably dispersed as an oil-water (O/W) emulsion in water, the emulsified oil in oily wastewater is difficult to remove using traditional methods (Zolfaghari et al., 2016). New and efficient oil removal techniques must be developed to eliminate the emulsified oil in O/W emulsions. Electro-demulsification provides several advantages: short treatment process, simple equipment, and minimal secondary pollution. The approach is widely used in the demulsification of water-in-oil emulsions but rarely in that of oil-in-water emulsions (Mohammadian et al., 2018; Mizoguchi & Muto, 2019; Yang et al., 2021; Li et al., 2023). The conductivity of the continuous phase of water-in-oil emulsions far exceeds that of O/W emulsions (Mhatre et al., 2015). When exposed to high electric fields, excessive current can flow through water-in-oil emulsions, leading to the electrolysis of the water phase within the emulsions (Peng et al., 2016; Ramadhan et al., 2023). Research on the electro-demulsification of O/W emulsions remains limited. However, an external electric field has been found to enhance the migration and redistribution of surface charges on oil droplets, lower the energy barrier at droplet surfaces, and accelerate the coalescence of these droplets.

Research has verified the feasibility of demulsification using electric fields to separate O/W emulsions (Ichikawa & Nakajima, 2004; Hosseini & Shahavi, 2012). In addition, studies have evaluated the effect of various parameters on electric field demulsification (Gong et al., 2019; Hu et al., 2021; Zhao et al., 2022). Findings on the coalescence of oil droplets in O/W emulsions indicate that a pulsed electric field exhibits application potential. Moreover, a variable pulsed electric field with specific intensity and frequency is superior to a constant pulsed electric field in promoting droplet coalescence. Studies on bidirectional direct current (DC) pulsed electric fields have also investigated the chaining and aggregation behavior of oil droplets in O/W emulsions (Ren & Kang, 2019). Research demonstrates that a bidirectional pulsed electric field outperforms both DC and alternating current electric fields in demulsification.

Several studies have simulated the dynamic response of droplets in low-viscosity fluids under pulsed DC and sinusoidal electric fields (Huang et al., 2020). In addition,

mathematical models have been established using user-defined functions to simulate the effect of coupled electric and flow fields on separating O/W emulsions (Wang et al., 2023). Molecular dynamics simulation has also been applied to assess the effect of DC electric fields on oil droplet motion, revealing negative electrophoretic migration (Qi et al., 2022). This method has been employed in other studies to investigate the effects of bidirectional pulsed electric fields on the transformation and aggregation behavior of oil droplets in emulsions. The results of these numerical simulations indicate that the oil droplets transformed and moved in the direction of the electric field (Liu et al., 2022). However, research has overlooked the use of the Lattice Boltzmann Method (LBM) to simulate the effect of bidirectional pulsed electric fields on the demulsification of emulsions.

Significant progress has been achieved in both experimental and theoretical research on pulsed electric field demulsification in recent years. Moreover, bidirectional pulsed electric field demulsification has proven to be an effective method (Tang et al., 2024). However, gaps persist in understanding the demulsification mechanism and the effects of bidirectional triangular pulsed electric fields on oil-in-water emulsions. The current study demonstrates the feasibility of using a bidirectional triangular pulsed electric field to separate oil-water emulsions and proposes an enhanced version of this technique. The findings presented in this study can be applied to the demulsification of water-in-oil emulsions, including the purification of O/W mixed emulsions in industrial processes and the treatment of oil-contaminated wastewater. In addition, this research contributes insights toward the advancement of more efficient demulsification technologies.

This study investigates the following aspects: 1) *Simulation of an O/W emulsion*. An O/W emulsion with 10% oil content is simulated by randomly generating droplets within the computational domain. The demulsification process is analyzed by changing the parameters of pulsed DC and unidirectional triangular pulsed electric fields. 2) *Development of an enhanced bidirectional triangular pulse*. An improved bidirectional triangular pulse based on the unidirectional triangular pulsed electric fields is developed, including multiple forward and reverse triangular pulse waves within a period. The evolution of the dilute emulsion is further simulated by adjusting pulse duration and electric field intensities. 3) *Assessment of droplet aggregation*. The aggregation behavior of oil droplets is evaluated using the ratio of total area to total perimeter.

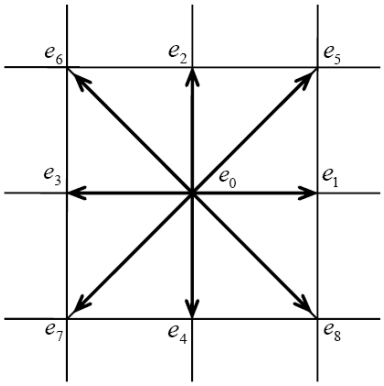

Fig. 1 D2Q9 lattice

2. THEORETICAL METHOD

2.1 Lattice Boltzmann Method for Oil-Water Phase Separation

The LBM models fluid motion through the evolution of mesoscopic particle distribution functions. This study employs a multiple-relaxation isothermal model, where the fluid is incompressible. The distribution functions in the LBM model are linked to lattice vectors. Thus, a two-dimensional nine-velocity (D2Q9) square lattice velocity model is used, as shown in Fig. 1.

$$\boldsymbol{c}_i = \begin{cases} (0,0) & i=0 \\ c(\cos(i-1)\frac{\pi}{2}, \sin(i-1)\frac{\pi}{2}) & i=1,2,3,4 \\ \sqrt{2}c(\cos(2i-1)\frac{\pi}{4}, \sin(2i-1)\frac{\pi}{4}) & i=5,6,7,8 \end{cases} \tag{1}$$

The calculation process is governed by the following two equations:

$$\rho\frac{\partial v}{\partial t} + \rho(v\cdot\nabla) = \nabla\cdot(-p\boldsymbol{I}+\tau) + F_{\mathrm{st}} + F_{\mathrm{E}} \tag{2}$$

$$\nabla\cdot v = 0 \tag{3}$$

The discrete evolution equation for the distribution function is given by

$$f_i(x+\boldsymbol{c}_i\delta_t, t+\delta_t) - f_i(x,t) = \Omega_{ki}(f_i^{eq}(x,t)) \tag{4}$$

where $f_i(x,t)$ represents the discrete velocity at time t and position x, δ_t is the time step, τ denotes the relaxation time, and $f_i^{eq}(x,t)$ indicates the distribution function in equilibrium.

The equilibrium state distribution function is expressed as

$$f_i^{eq} = \omega_i\rho(1+\frac{3}{w_i}\boldsymbol{c}_i\boldsymbol{u}+\frac{9}{2w_i^4}(\boldsymbol{c}_i\boldsymbol{u})^2-\frac{3}{2w_i^2}\boldsymbol{u}^2) \tag{5}$$

where w_i is the weight coefficient.

$$w_i = \begin{cases} 4/9 & i=1 \\ 1/9 & i=2,3,4,5 \\ 1/36 & i=6,7,8,9 \end{cases} \tag{6}$$

In this study, the dynamic current caused by the electric field is negligible; thus, the model ignores the effects of magnetic forces. The relationship between electric field strength and potential can be expressed as

$$\mathrm{E} = -\nabla\Phi \tag{7}$$

The charge conservation equation for the fluid is given by

$$\nabla \cdot (\sigma E) = 0, \nabla \cdot (\sigma \nabla \Phi) = 0 \tag{8}$$

Using the Maxwell stress tensor to represent the electric field force on the droplet yields

$$F_{\mathrm{E}} = \nabla(\varepsilon_{\mathrm{b}}\varepsilon_{\mathrm{r}} EE) - \frac{1}{2}E^2 \nabla \varepsilon_{\mathrm{b}}\varepsilon_{\mathrm{r}} = \nabla \cdot \mathrm{T} \tag{9}$$

where ρ, v, p, I, τ, and F represent fluid density, fluid velocity, pressure, identity matrix, viscous shear stress tensor, and interfacial tension, respectively. F_{E} denotes the physical force or electric field force in this article, σ represents the conductivity, and ε is the dielectric constant.

2.2 Color Model in the Lattice Boltzmann Method for Phase Separation

The LBM color model, first proposed by Gunstensen et al. (1991), uses different colors to represent different fluid phases. Each phase has a distribution function representing the evolution of particles within different fluids. The model uses color gradients to represent the interactions between different fluids. However, this approach does not ensure the two phases of the fluid are mutually insoluble. To address this issue, Latva-Kokko and Rothman (2005) introduced a recoloring algorithm that facilitates the separation of the two fluids while maintaining isotropy at the phase interface and effectively reducing pseudo-velocity at that interface.

Let water be the continuous phase (denoted by the subscript "*b*," shown in blue) and oil droplets the dispersed phase (denoted by the subscript "*r*," shown in red), with *k*=*b* or *r*. In Equation (4), also known as the evolution equation, (the collision operator $\Omega_{ki}(x,t)$ consists of three operators:

$$\Omega_{ki}(x,t) = \Omega_{ki}^{3}(x,t)(\Omega_{ki}^{1}(x,t) + \Omega_{ki}^{2}(x,t)) \tag{10}$$

where $\Omega_{ki}^{1}(x,t)$ represents the single-phase collision operator, which describes the mutual collision behavior of particles within the two fluids. It is expressed as

$$\Omega_{ki}^{1}(x,t) = f_{ki}(x,t) - \tau(f_{ki}(x,t) - f_{ki}^{(\mathrm{eq})}(x,t)) \tag{11}$$

where τ represents the relaxation factor, and $f_i^{eq}(x,t)$ is the equilibrium distribution function given by

$$f_{ki}^{eq} = \rho_k(\varphi_i^k + \omega_i(1 + \frac{3}{w_i}\boldsymbol{c}_i\boldsymbol{u} + \frac{9}{2w_i^4}(\boldsymbol{c}_i\boldsymbol{u})^2 - \frac{3}{2w_i^2}u^2)) \tag{12}$$

and

$$\rho_k = \sum_i f_{ki} \tag{13}$$

$$\boldsymbol{u} = \frac{1}{\rho}\sum_i\sum_k f_{ki}\boldsymbol{c}_i \tag{14}$$

φ_i^k is a function of α_k, where α_k is a free parameter

$$\varphi_i^k = \begin{cases} \alpha_k & i = 1 \\ (1-\alpha_k)/5 & i = 2,3,4,5 \\ (1-\alpha_k)/20 & i = 6,7,8,9 \end{cases} \tag{15}$$

$\Omega_{ki}^{2}(x,t)$ is the interface perturbation operator representing the interactions caused by interfacial tension within the interface region of the two fluid phases. Let F denote the color gradient at the interface, expressed as

$$F(x) = \sum_{\mathrm{i}} \boldsymbol{c}_i(\rho_r(x+\boldsymbol{c}_i) - \rho_b(x+\boldsymbol{c}_i)) \tag{16}$$

Therefore, the perturbation operator is given as

$$\Omega_{ki}^{2}(\mathrm{x,t}) = \frac{A_{\mathrm{K}}}{2}|F|(W_i\frac{(F\cdot c_i)^2}{|F|^2}) - B_i \tag{17}$$

$$B_i = \begin{cases} -4/27 & i = 1 \\ 2/27 & i = 2,3,4,5 \\ 5/108 & i = 6,7,8,9 \end{cases} \tag{18}$$

$\Omega_{ki}^{3}(x,t)$ is the recoloring operator that ensures particles in the phase interface region do not enter the phase region of one another. Leclaire et al. (2013), building upon Reis and Phillips (2007), expanded the model for immiscible multiphase fluids. This model is applicable to fluids with high density and viscosity ratios. This study also adopts this simplified model. The equation for the recoloring operator is as follows

$$\Omega_{ri}^{3}(f_{ri}) = \frac{\rho_r}{\rho}f_i + \beta\frac{\rho_r\rho_b}{\rho^2}\cos(\varphi_i)\Sigma_k f_{ki}^{e}(\rho_k, 0, \alpha_k) \tag{19}$$

$$\Omega_{bi}^{3}(f_{bi}) = \frac{\rho_r}{\rho}f_i - \beta\frac{\rho_r\rho_b}{\rho^2}\cos(\varphi_i)\Sigma_k f_{ki}^{e}(\rho_k, 0, \alpha_k) \tag{20}$$

2.3 Boundary Condition

In this study, a periodic boundary treatment is applied in the Y-direction, allowing particles to exit the flow field from one boundary and enter from the opposite boundary at the next time step. Meanwhile, a bounce-back scheme is used in the X-direction, where particles rebound in the opposite direction after colliding with the boundary. In this method, boundary particles do not participate in collisions, and the distribution function at boundary points is determined by adjacent lattice points after the collision.

In the X direction, there is:

$$f_3(x,0) = f_3(x \pm 1, 0) \tag{21}$$

$$f_1(x,0) = f_3(x,0) \tag{22}$$

In the Y direction, there is:

$$f_{2,5,6}(x,0) = f_{2,5,6}(x, N_y) \tag{23}$$

$$f_{4,7,8}(x,0) = f_{4,7,8}(x,1) \tag{24}$$

2.4 Pulse Voltage Formula

The DC pulse voltage is set with a duty cycle of 50% within each period, expressed as

$$U_1 = \begin{cases} U, 0 < t < T/2 \\ 0, T/2 < t < T \end{cases} \tag{25}$$

U_1 represents the value of the DC pulse voltage at time *t*, U is the value of the DC voltage, and T denotes the period of the DC pulse voltage. The duty ratio is expressed as $n = T_f / T$, where T_f is the part of the cycle corresponding to $U_1 = U$.

For the unidirectional triangular pulse voltage established in this study,

$$U_2 = \begin{cases} kt, 0 < t < T/2 \\ -kt + 2U_{max}, T/2 < t < T \end{cases} \tag{26}$$

where U_2, U_{max} and T represent the voltage value, maximum voltage value, and period of unidirectional triangular pulse at time t, respectively. k is the slope related to the maximum voltage U_{max} and period T, given by $k = 2U_{max}/T$.

Based on the unidirectional triangular pulse electric field, an improved bidirectional triangular pulse electric field is defined as follows:

$$U_3 = \begin{cases} U_2, 0 < t < T_0/2 \\ -U_2, T_0/2 < t < T_0 \end{cases} \tag{27}$$

U_3, U_2, and T_0 denote the voltage, the unidirectional triangular pulse voltage from Equation (27), and the total cycle period of the bidirectional triangular pulse at time *t*, respectively. Notably, one cycle period may include one or more unidirectional triangular pulse waveforms.

3. SIMULATION RESULTS AND DISCUSSION

The parameters used in this simulation are dimensionless parameters of crude oil, providing new insights for the treatment of oily wastewater. However, the effect of gravity on the demulsification process is not considered in this study. In practical applications, gravity can influence the motion dynamics of oil droplets in the emulsion.

This study adopts an isothermal incompressible model. In actual demulsification processes, temperature often fluctuates, affecting the properties of oil droplets (such as viscosity and conductivity).

In addition, computers cannot accurately simulate the random distribution of oil droplets in the emulsion, potentially leading to uneven distribution of oil droplets during demulsification. These factors may contribute to discrepancies between simulation results and real processes.

This study employs a computational grid of 256×256 uniform cells, with the electric field direction set from top to bottom (y direction), while neglecting the influence of gravity. At the initial stage, the simulation models an oil-in-water emulsion with an oil content of approximately 10% through program writing and settings. The nondimensionalized parameters s_1, t_1, U_1,and σ_1 denote the actual length, time, voltage, and interfacial tension coefficient, respectively. Meanwhile, s, t, U, and σ_0 represent the nondimensionalized length, time, voltage, and interfacial tension coefficient, where $s_1 = s \times 10$, $t_1 = t/10^3$, $U = U_1/U_2$,and $\sigma_0 = \sigma_1/\sigma_2$. U_2 and σ_2 represent the unit voltage and unit interfacial tension coefficient, respectively. ρ_r and ρ_b denote the nondimensionalized densities of the oil droplets and water, respectively. ε_r^1 and ε_b^1 represent the actual dielectric constants, whereas ε_r and ε_b are the nondimensionalized dielectric constants for the oil droplets and water, respectively. Thus,

$$\varepsilon_r = \sqrt{\frac{\varepsilon_r^1}{\varepsilon_r^1 + \varepsilon_b^1}}, \varepsilon_b = \sqrt{\frac{\varepsilon_b^1}{\varepsilon_r^1 + \varepsilon_b^1}} \tag{28}$$

σ_r^1 and σ_b^1 denote the actual electrical conductivities of oil and water, respectively, whereas σ_r and σ_b represent the nondimensionalized electrical conductivities of the oil and water, respectively. Thus,

$$\sigma_r = \sqrt{\frac{\sigma_r^1}{\sigma_r^1 + \sigma_b^1}}, \sigma_b = \sqrt{\frac{\sigma_b^1}{\sigma_r^1 + \sigma_b^1}} \tag{29}$$

η_r^1 and η_b^1 are the actual viscosities of the oil droplets and water, respectively, whereas η_r and η_b represent the nondimensionalized viscosities of the oil and water, respectively. The relationship can be expressed as follows:

$$\eta_r = \sqrt{\frac{\eta_r^1}{\eta_r^1 + \eta_b^1}}, \quad \eta_b = \sqrt{\frac{\eta_b^1}{\eta_r^1 + \eta_b^1}} \tag{30}$$

In this study, the parameters for the oil droplets are set to typical values for crude oil, with the nondimensionalized parameters configured as follows: $s = 1$, $t = 1$, $\sigma_0 = 0.018$, $\varepsilon_r = 0.0019$, $\varepsilon_b = 0.0098$, $\sigma_r = 0.41$, $\sigma_b = 0.91$, $\rho_r = 0.9$, $\rho_b = 1$, $\eta_r = 0.87$, $\eta_b = 0.47$. And these are shown in Table 1.

Table 1 The actual and Nondimensionalized parameters of oil and water.

Actual parameters	density	dielectric constant	electrical conductivity	viscosity
Oil	$0.9 kg/m^3$	3F/m	$2\times10^{-4} S/m$	$0.01 Pa \cdot s$
Water	$1.0 kg/m^3$	78F/m	$1\times10^{-3} S/m$	$0.00298 Pa \cdot s$
Nondimensionalized parameters	density	dielectric constant	electrical conductivity	viscosity
Oil	0.9	0.0019	0.41	0.87
Water	1.0	0.0098	0.91	0.47

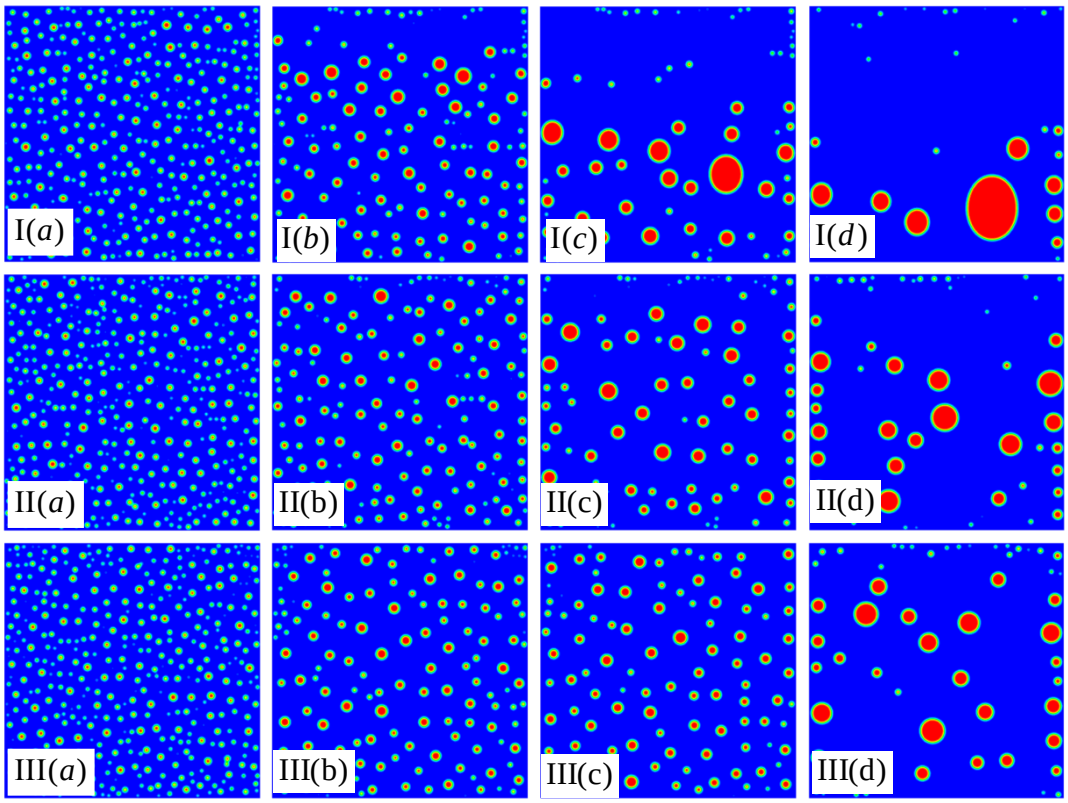

Fig. 2 Evolution chart of emulsion in pulsed electric field at V=100. $I(a)t=1\times10^4$, $I(b)t=1\times10^5$, $I(c)t=4\times10^5$, $I(d)t=1.4\times10^6$ **for** $T=10^3$, $II(a)t=1\times10^4$, $II(b)t=1\times10^5$, $II(c)t=4\times10^5$, $II(d)t=1.4\times10^6$ **for** $T=10^4$, $III(a)t=1\times10^4$, $III(b)t=1\times10^5$, $III(c)t=4\times10^5$, $III(d)t=1.4\times10^6$ **for** $T=10^5$

3.1 Effect of DC Pulsed Electric Fields on Demulsification in Dilute Emulsions

In this section, DC pulsed electric fields with different periods were established. The voltage V all set to 100, with a duty ratio ***n*** of 50%. The direction of the electric field was oriented from top to bottom.

The results in Fig. 2 are summarized as follows: 1) In the initial stages, oil droplets in the dilute emulsion migrate from top to bottom in the direction of the electric field. The reason is that owing to the different velocities of the oil droplets, collisions may occur between them during their movement, leading to the aggregation and formation of larger oil droplets. 2) When $T=10^3$, the high frequency of the electric field force exceeds the surface tension of the oil droplets. Consequently, the oil droplets become elliptical in the direction of the electric field, shortening the distance between the oil droplets and rendering them prone to aggregation. 3) When $T=10^4$ and $T=10^5$, the lower frequency of the electric field force results in a slight change in the shape of the oil droplets, retaining its approximately circular form. Consequently, the oil droplet aggregation rate decreases under the action of these two electric field periods.

The frequency of the electric field affects the oil droplet aggregation rate across the three periods studied. Shorter periods lead to faster and more concentrated aggregation, whereas longer periods indicate slower and more dispersed aggregation.

3.2 Influence of Unidirectional Triangular Pulsed Electric Field on Demulsification in Dilute Emulsion

Figure 3 illustrates the effect of triangular pulsed electric fields at different voltages on the demulsification of O/W emulsions, with control voltages after nondimensionalization set to V=100, V=300, and V=500. The period of the triangular pulsed electric field was set at 100 for all cases, with the electric field oriented from top to bottom.

The evolution of the emulsion under unidirectional triangular pulsed electric fields is described as follows: 1) After the application of the triangular pulsed electric field, oil droplets in the upper half move downward in the directionof the electric field, colliding and aggregating with other oil droplets during their movement. 2) When the oil droplets move downward and formed larger droplets, the effect of the electric field force weakens, causing the droplets to sotp moving downward and instead aggregate laterally. 3) As the voltage increases, the effect of the electric field force on the oil droplets also intensifies. The surface tension of the oil droplets is less than the electric field force; thus, the droplets become more noticeably deformed as the electric field force increases. The shape of the oil droplets is nearly circular at V=100. Meanwhile, the oil droplets transform into an ellipse with a longer major axis as the voltage increases to V=300. At V=500, the effect of the electric field force on the oil droplets markedly exceeds that of surface tension, causing the oil droplets to become elongated into a strip-like form. 4) After small droplets aggregate into a

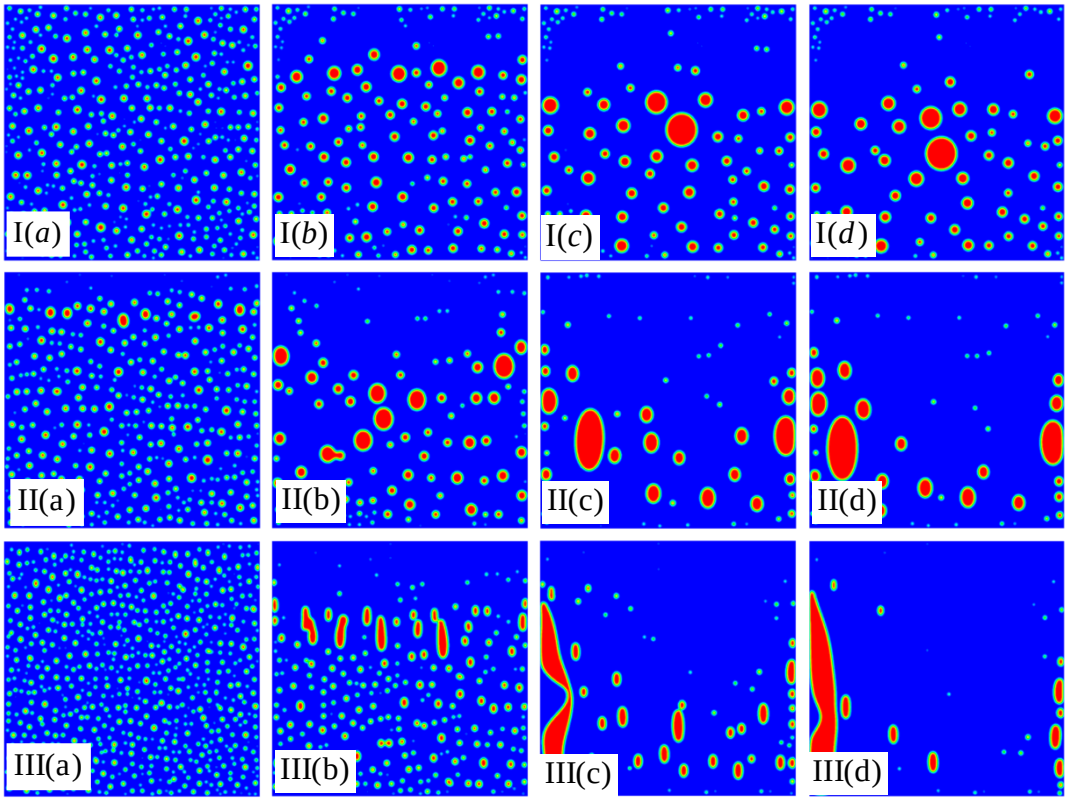

Fig. 3 Evolution of dilute emulsion under unidirectional triangular pulsed electric field with varying field strengths, maintaining a period of 100 for all cases. $\mathrm{I(a)t=0}$, $\mathrm{I(b)t=6\times10^4}$, $\mathrm{I(c)t=2\times10^5}$, $\mathrm{I(d)t=4\times10^5}$ **for** $\mathrm{V=100}$, $\mathrm{II(a)t=0}$, $\mathrm{II(b)t=5\times10^4}$, $\mathrm{II(c)t=1.7\times10^5}$, $\mathrm{II(d)t=4\times10^5}$ **for** $\mathrm{V=300}$, $\mathrm{III(a)t=0}$, $\mathrm{III(b)t=2\times10^4}$, $\mathrm{III(c)t=9\times10^4}$, $\mathrm{III(d)t=1.4\times10^5}$ **for** $\mathrm{V=500}$

large area of oil droplets, the shape of the oil droplets presents a pointed top, a concave middle, and a bottom resembling an elliptical strip. Moreover, the oil droplets tend to rupture in the middle, forming two droplets and a concave appearance in the middle of the oil droplets. This occurrence is attributed to the considerably greater electric field force than the surface tension.

Under the unidirectional triangular pulsed electric field, an increase in voltage leads accelerates the movement of the oil droplets in the dilute emulsion. Higher voltage also increases droplet deformation, increasing the probability of contact between droplets. Therefore, as voltage rises, demulsification efficiency improves. However, excessively high voltage can potentially cause oil droplets to fragment into smaller ones.

3.3 Effect of Bidirectional Triangular Pulsed Electric Field on Demulsification in Dilute Emulsions

The electric field direction was first defined as top-to-bottom for positive and bottom-to-top for negative. Based on the unidirectional triangular pulsed electric field, a bidirectional triangular pulsed electric field was established, incorporating both positive and negative pulses. Within a cycle, the first half consists of a positive triangular pulsed electric field, and the second half consists of a negative triangular pulsed electric field. Both positive and negative triangular pulsed electric fields have a period of 100. This cycle is denoted as T in this study.

3.3.1 Demulsification Efficiency in Dilute Emulsions under Bidirectional Pulsed Electric Field with Different Electric Field Intensities

Figure 4 shows the effect of varying electric field strengths on the oil droplet aggregation rate under a bidirectional triangular pulsed electric field, as follows: 1) The positive triangular pulsed voltage is applied first, causing the oil droplets to move from the top to the bottom under the influence of the electric field force, as well as collide and aggregate with other oil droplets during their motion. The changes in the direction of the triangular pulsed electric field led to an increase in the electric field force on the oil droplets at the bottom of the flow field. Meanwhile, the decrease in the electric field force at the top of the flow field resulted in the lower droplets moving upward. 2) Simultaneously, the frictional resistance of oil droplets moving in water increases under the influence of viscosity because of the earlier formation of larger oil droplets at the top. Consequently, the upward movement of the upper oil droplets slows down. Therefore, an increase in collision probability and aggregation efficiency is observed between the lower and upper oil droplets. 3) After small oil droplets aggregate into larger ones, their gathering through vertical movement decreases. The shape of the oil droplets changes periodically in the direction of the electric field (between circular and approximately elliptical). This change in shape increases the probability of contact with nearby oil droplets on both sides. At this stage, the oil droplets exhibit a trend of movement and aggregation toward the left and right sides of the flow field.

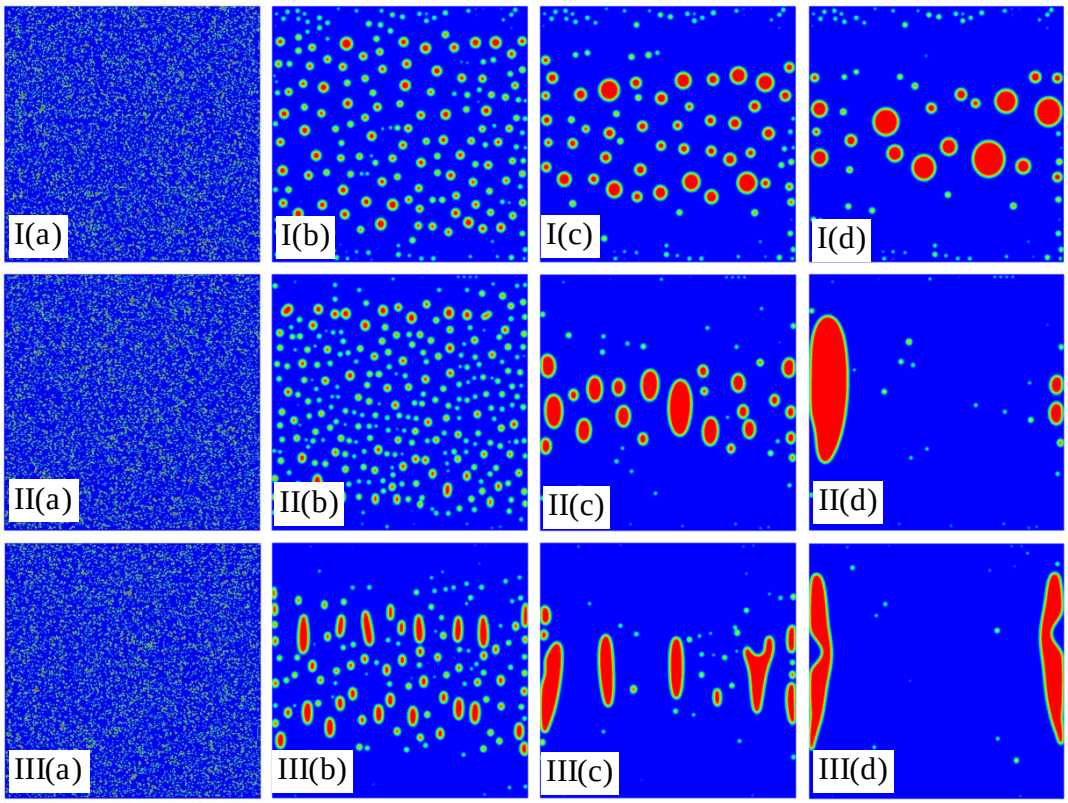

Fig. 4 Evolution chart of dilute emulsions under bidirectional triangular pulsed electric fields with varying intensities $T=10^4$. $I(a)t=0$, $I(c)t=5\times10^4$, $I(c)t=2\times10^5$, $I(d)t=4\times10^5$ **for** $V=100$, $II(a)t=0$, $II(b)t=1\times10^4$, $II(c)t=7\times10^4$, $II(d)t=1.8\times10^5$ **for** $V=300$, $III(a)t=0$, $III(b)t=1.5\times10^4$, $III(c)t=4\times10^4$, $III(d)t=7\times10^4$ **for** $V=500$

The results shown in Fig. 4 reveal similarities and differences. 1) Before the oil droplets aggregate in the middle of the flow field to form larger droplets, an increase in electric field strength leads to an increase in electric field force. This occurrence promotes oil droplet aggregation in the direction of the electric field. By contrast, the degree of aggregation decreases in the direction perpendicular to the electric field. Consequently, a more uniform distribution of large oil droplets is observed in the middle of the flow field as the electric field strength increases, as shown in Fig. 4. III(c). 2) In Fig. 4, the oil droplets aggregate with nearby droplets perpendicular to the direction of the electric field. Consequently, a more uneven distribution of oil droplets is observed in the middle of the flow field after aggregation, at lower electric field strengths. 3) The distribution of oil droplets in the middle of the flow field determines the size of the oil bands on both the left and right sides of the flow field thereafter. For instance, at V=300, the oil droplets exhibit an uneven distribution in the middle of the flow field, with more oil droplets gathering on the left side. This occurrence resulting in the formation of a single oil band on the left side of the flow field. However, at V=500, the oil droplets exhibit a relatively uniform distribution in the middle of the flow field, with two oil bands of similar size forming on both sides.

3.3.2 Dilute Emulsion Demulsification Using Bidirectional Triangular Pulses with Varying Periods (T)

Figure 5 illustrates the effects of varying periods (T) on the demulsification evolution of a dilute emulsion, under the control of a bidirectional triangular pulsed electric field. The electric field intensity remains constant across all three T periods.

The evolution of the emulsion shows the following: 1) At T=200, the electric field contains only one positive and one negative triangular pulse waveform within each period T, hence the rapid change in the direction of the electric field, as shown in Equation (28). When the oil droplet area is small, the viscous force between the droplets and water is less than the electric field force acting on the droplets. The droplets then move periodically in the direction of the electric field because of the regular shifts in direction. This pattern reduces the probability of droplet contact in the direction of the electric field, thus decreasing the droplet aggregation rate. 2) However, as shown in Figures I(b) and II(b), the displacement of droplets within one period T exceeds that at T=200 because of the inclusion of multiple positive and negative triangular pulse waveforms when $T=10^3$. At the same stage of emulsion evolution as T=200, larger droplets formed at $T=10^3$ are closer to the center of the flow field, hence the earlier formation of large oil bands. The result suggests that the low-frequency change in the direction of the electric field allows droplets to move farther in one direction in the early stages. Consequently, the probability of droplet contact in the direction of the electric field rises, resulting in an increase in droplet aggregation rate. 3) Moreover, an increase in viscous force delays the movement of a larger droplet. At this point, the low-frequency changes lead to a reduced frequency of droplet deformation in the direction of the electric field. The electric field forces ease the deformation

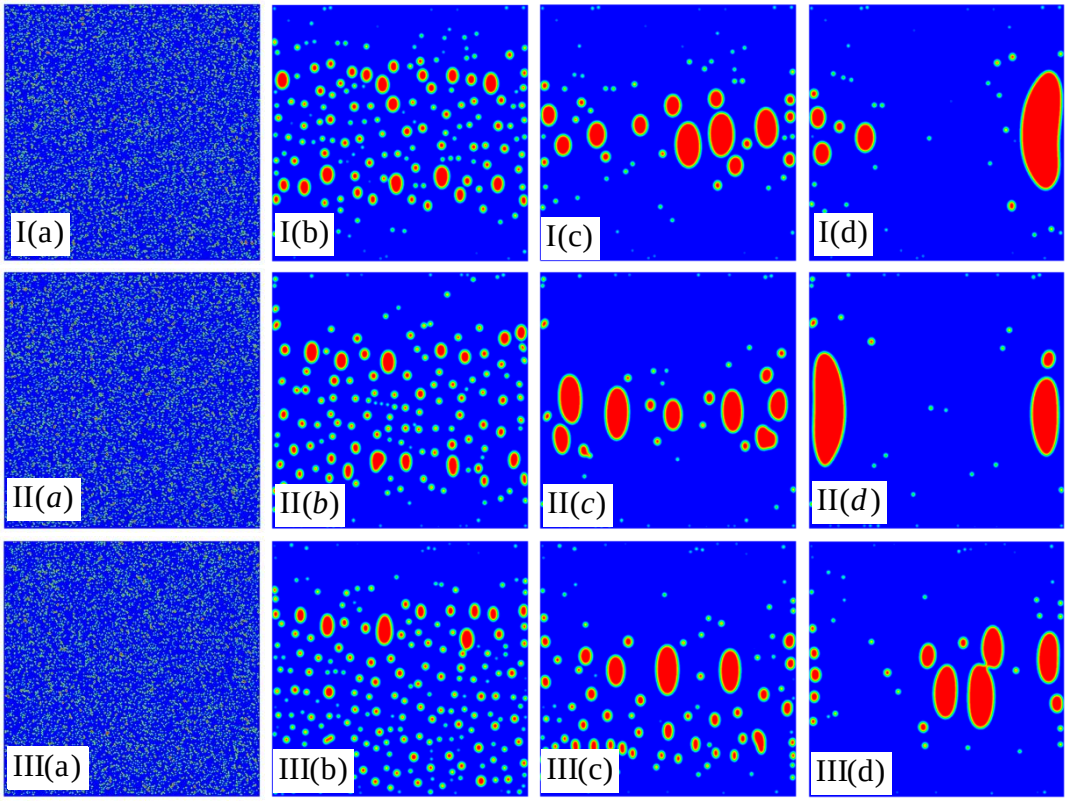

Fig. 5 Evolution chart of dilute emulsion under bidirectional triangular pulsed electric fields with varying periods T at $V=300$. I(a)$t=0$, I(b)$t=2\times10^4$, I(c)$t=7\times10^4$, I(d)$t=1.2\times10^5$ **for** $T=2\times10^2$, II(a)$t=0$, II(b)$t=2\times10^4$, II(c)$t=7\times10^4$, II(d)$t=1.2\times10^5$ **for** $T=10^3$, III(a)$t=0$, III(b)$t=2\times10^4$, III(c)$t=5.6\times10^4$, III(d)$t=1.2\times10^5$ **for** $T=10^5$

of large oil droplets, promoting further merging into even larger oil droplets. Consequently, the droplet aggregation rate decreases, as shown in Figs. I(d), II(d), and III(d). The time required for the droplets to form oil bands is prolonged at $T=10^5$, relative to T=200 and $T=10^3$.

The results indicate that the size of the period T affects the droplet aggregation rate by modulating droplet displacement. The initial aggregation rate is higher with a larger T; however, the time required for droplets to aggregate into oil bands is extended at lower frequencies of droplet deformation.

3.3.3 Evolution of Dilute Emulsion with Different Component Ratios Under the Control of Bidirectional Triangular Pulsed Electric Field

Figure 6. investigates the evolution of demulsification of a dilute O/W emulsion under a bidirectional triangular pulsed electric field, with O/W component ratios of 5% and 20%.

The oil droplets are more dispersed in the emulsion with 5% oil but denser in that with 20% oil. Thus, the aggregation rate of the oil droplets is higher in the 20% emulsion than in the 5% emulsion. This difference is attributed to the higher probability of droplet contact under the electric field force with 20% oil. Compared with the evolution trend of the oil droplets in the emulsion, both types of emulsions exhibit similar aggregation behavior: 1) Oil droplets move toward the central part of the flow field from the upper and lower regions under the influence of the bidirectional triangular pulsed electric field. 2) After larger oil droplets form in the middle of the flow field, they move toward the left and right sides of the flow field, eventually forming oil bands.

The results in Fig. 6 indicate that the bidirectional triangular pulsed electric field effectively demulsifies dilute emulsions with higher oil content while maintaining effectiveness for those with lower oil component ratios.

3.3.4 Analysis of the Demulsification Principle of Bidirectional Triangular Pulsed Electric Fields

Figure 7. illustrates the evolution of streamlines under the influence of a bidirectional triangular pulsed electric field. When the direction of the electric field first changes, the distribution of the majority of streamlines is uniform, as shown in I(a). The change in the flow field lags behind the change in the electric field, hence at this time the direction of the streamlines is opposite to the direction of the electric field. The variation in the electric field direction leads to a redistribution of charges on the surface of the oil droplets, and the electric field force prompts the oil droplets to begin moving in the opposite direction of the streamlines. This effect disturbs the velocity distribution in the flow field, creating unevenly distributed vortices, as shown in I(b) and I(c). Under the continuous action of the electric field force, the streamlines gradually return to a uniform distribution. Meanwhile, the flow field repeats the previous process after the next change in the electric field direction, as shown in I(d).

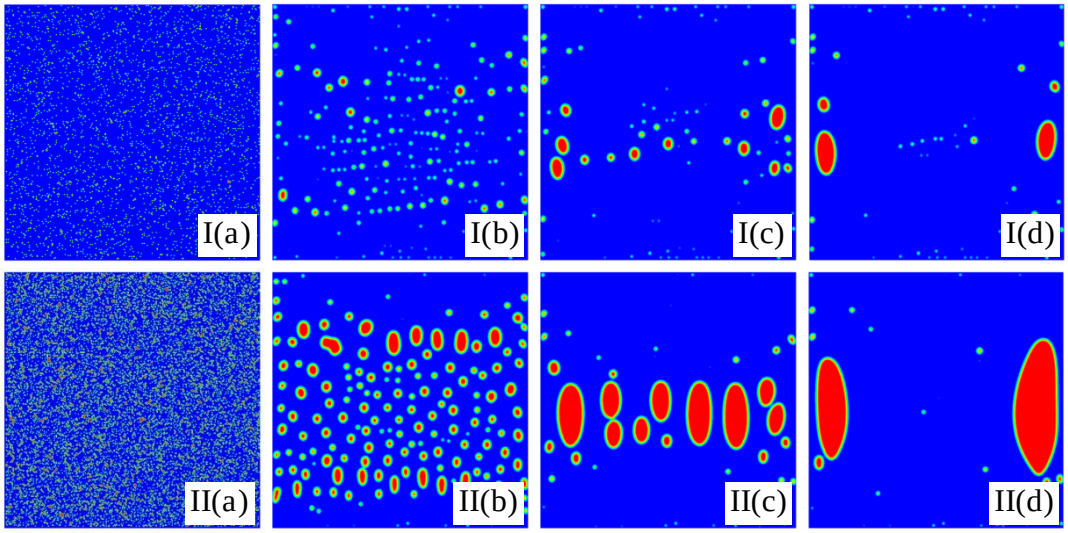

Fig. 6 Evolution chart of dilute emulsions with varying oil-to-water ratios under bidirectional triangular pulsed electric field at different periods. Component ratios examined are as follows: $V = 300$ **and** $T = 1\times10^{3}$. $I(a)t = 0$, $I(b)t = 4\times10^{4}$, $I(c)t = 1.5\times10^{5}$, $I(d)t = 2.3\times10^{5}$ **at an oil-in-water ratio of** 5%; $II(a)t = 0$, $II(b)t = 1\times10^{4}$, $II(c)t = 5\times10^{4}$, $II(d)t = 9\times10^{4}$ **at an oil-in-water ratio of** 20%

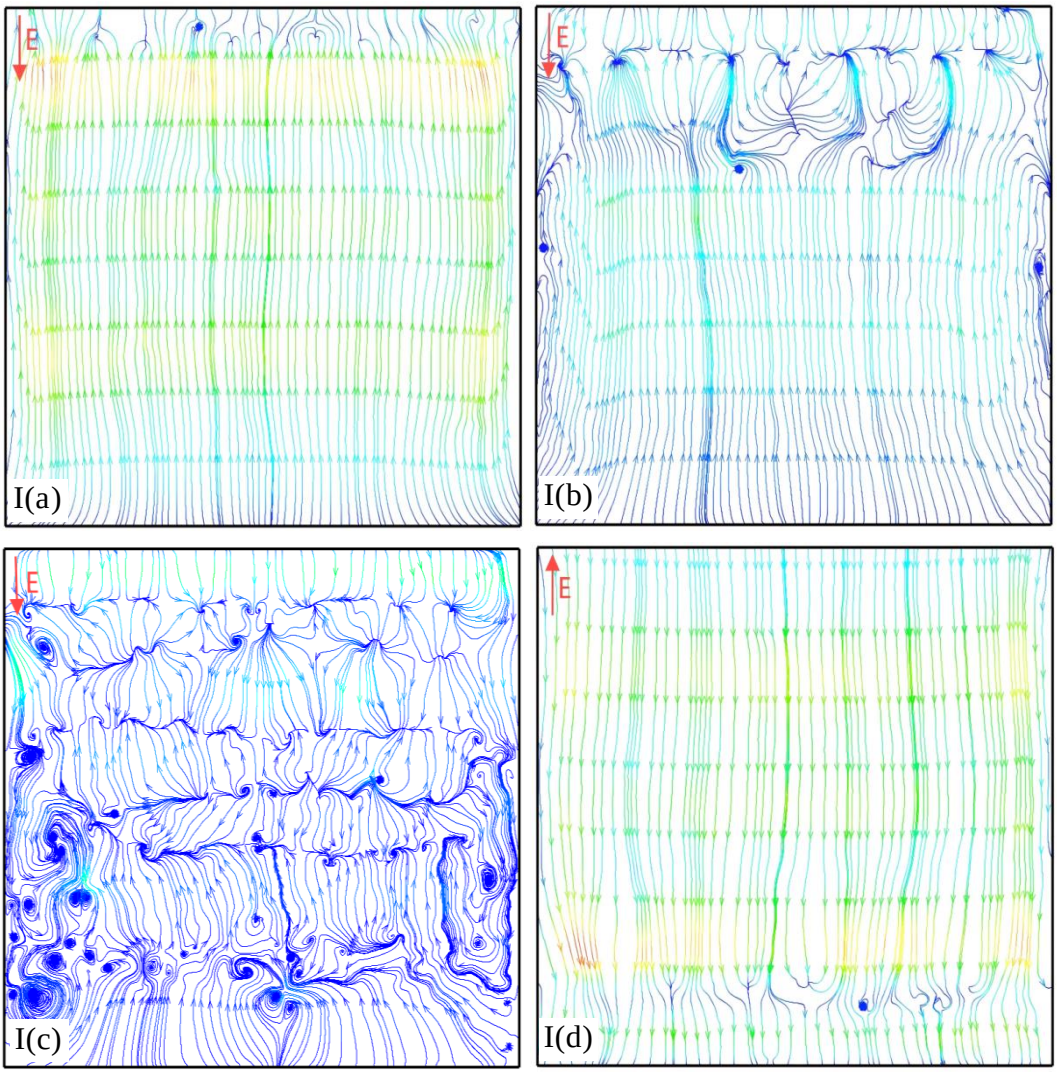

Fig. 7 shows the evolution of the flow field under the action of a bidirectional triangular pulsed electric field, with E representing the direction of the electric field. And t represents the time step, for I(a) $t = 1.1\times10^{4}$**, I(b)** $t = 1.4\times10^{4}$**, I(c)** $t = 1.5\times10^{4}$**, I(d)** $t = 1.6\times10^{4}$

The phenomena demonstrate that the changes in the flow field exhibit a lag, which increases the probability of collisions between oil droplets. Meanwhile, the vortices generated in the flow field promote the aggregation of oil droplets. Moreover, the vortices are more abundant on both sides of the flow field, which ultimately leads to a trend of oil droplet aggregation perpendicular to the direction of the electric field.

3.4 Conclusion from Simulation Results

Under a pulsed electric field, oil droplets generate internal polarized charges. The distribution of these polarized charges at the ends of the oil droplets subjects them to the electric field force. Consequently, the droplets move from regions of high to low electric potential in the direction of the electric field. This movement increases the probability of collisions between oil droplets. The simulation results indicate the following:

a) Oil droplets move in a single direction under the action of DC and unidirectional triangular pulsed electric fields. In regions of low electric potential, the electric field force weakens, prompting a decrease in the efficiency of oil droplet aggregation. However, with bidirectional triangular pulsed electric fields, periodic changes in the direction of the electric field cause variations in the electric field force. Consequently, oil droplets at both ends of the flow field move toward the center, resulting in a high probability of collisions. Therefore, the efficiency of oil droplet aggregation under bidirectional triangular pulsed electric fields is higher than that under the first two types of electric fields.

b) After polarization by the electric field, opposite charges accumulate at the ends of the oil droplets. Consequently, forces act in opposite directions at each end, causing droplet deformation in the direction of the electric field. When the electric field strength is excessively high and continues to act on the oil droplets, it can cause the droplets to split. This effect can be mitigated using the bidirectional triangular pulsed electric field discussed in this study. The periodic changes in the direction of the electric field allow the redistribution of polarized charges on the surface of the oil droplets, preventing prolonged exposure to excessive electric field forces. Thus, compared with other methods, the bidirectional triangular pulsed electric field proposed in this study can use a higher electric field strength to achieve greater demulsification efficiency.

4. QUANTITATIVE ANALYSIS OF DEMULSIFICATION EFFICIENCY IN EMULSIONS UNDER PULSED ELECTRIC FIELD

Under the electric field, oil droplets exhibit electrophoretic and oscillatory coalescence, increasing in size and periodically changing shape in the direction of the electric field. The emulsion contains numerous oil droplets; thus, tracking the area and morphological changes of each droplet would be computationally intensive. In this study, the oil droplet aggregation rate and morphological changes are analyzed by calculating the ratio of the total area to the collective perimeter, as follows:

$$D_r = \frac{S_r}{L_r} \tag{31}$$

where D_r is the ratio of the total area to the total perimeter of the oil droplets, S_r denotes the total area of the oil droplets, and L_r represents the total perimeter of the oil droplets.

During the aggregation of two oil droplets, the total surface area of the two droplets remains constant, while the total perimeter increases. This behavior leads to an increase in D_r, indicating that this trend can reflect the degree of oil droplet aggregation.

The rising trend of D_r indicates that oil droplet aggregation is dominant at the given time. When aggregation is completed, the oil droplet deform because of the electric field force. This effect alters the perimeter of the droplets, but the area of the oil droplets remains unchanged.

At this stage, the change in D_r denotes the extent of shape change in the oil droplets: a smaller D_r indicates a greater degree of shape change. Thus, the change in D_r allows the quantitative analysis of the aggregation behavior and shape changes of oil droplets at different stages.

4.1 Quantitative Analysis of Demulsification Efficiency in Emulsions Under Different Pulsed Electric Fieldss

As shown in Fig. 8, the D_r value of oil droplets changes under different pulsed electric fields, where $T = 10^3$ and V=100.

Within the time step from $t = 0 \sim 5\times10^4$, the changes in D_r are similar under the three pulsed electric fields, indicating the identical demulsification efficiency of the three pulsed electric fields on the emulsion at this stage. Between $t = 5\times10^4 \sim 3\times10^5$, the change in D_r for the DC pulsed electric field exceeds that for the other two fields, suggesting that the demulsification efficiency of the DC pulsed electric field is superior to that of the other two fields during this phase.

At the time point $t = 10^5$, the rate of change in D_r for the bidirectional triangular pulsed electric field exceeds that for the unidirectional triangular pulsed electric field and continues to rise in the subsequent stages. At $t = 3\times10^5$, the rate of change in D_r for the bidirectional triangular pulsed electric field surpasses that for the DC pulsed electric field; meanwhile, the increase in D_r for the unidirectional triangular pulsed electric field remains relatively low.

Quantitative results indicate the following: a) In the initial stages of emulsion evolution, the three pulsed electric fields exert comparable demulsification efficiency; in the intermediate stage, the DC pulsed electric field performs better than the others; however, in the later stage, the DC pulsed electric field is less effective than the bidirectional triangular pulsed electric field. b) The unidirectional triangular pulsed electric field exhibits a consistently low oil droplet aggregation rate. The demulsification efficiency of this electric field on the emulsion is inferior to the effects of the other two fields. c) The bidirectional triangular pulsed electric field demonstrates superior demulsification efficiency in the emulsion, with a higher degree of oil droplet aggregation.

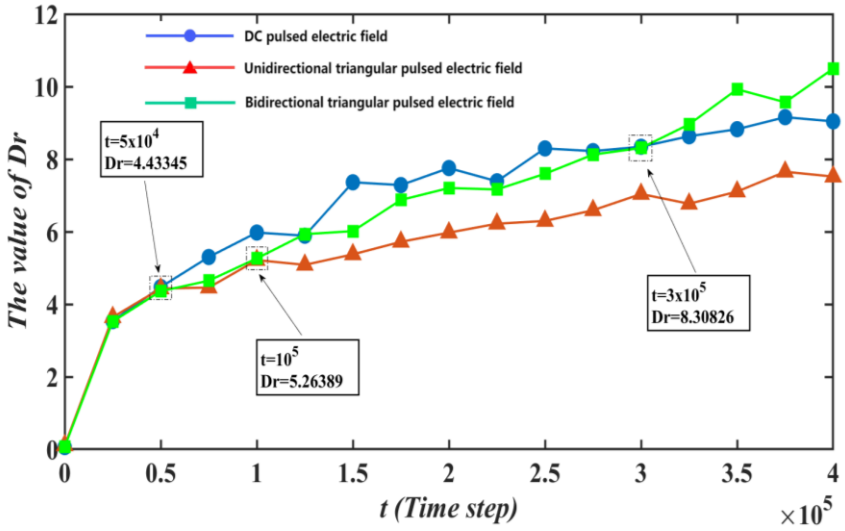

Fig. 8 Variations in D_r of emulsions under different pulsed electric fields at $T=10^3$ and $V=100$: (a) DC pulsed electric field, (b) Unidirectional triangular pulsed electric field, and (c) Bidirectional triangular pulsed electric field

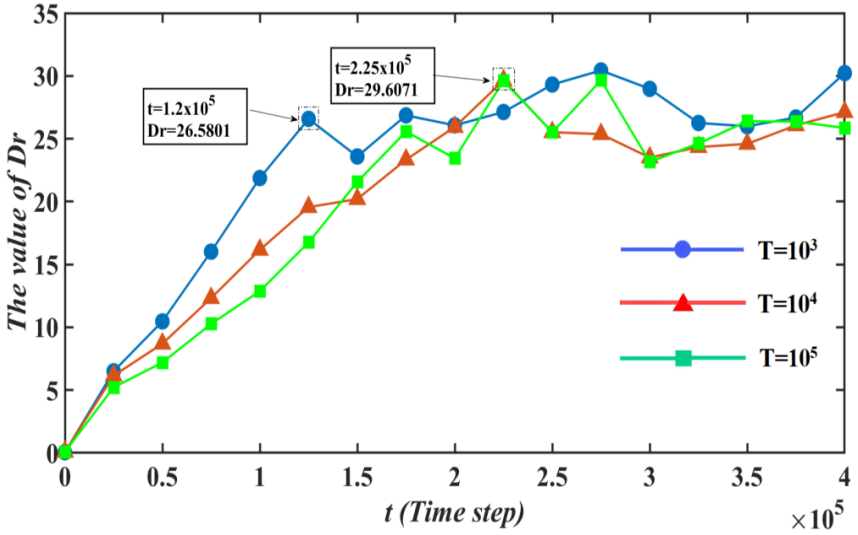

Fig. 9 Variations in D_r of emulsions under bidirectional triangular pulsed electric fields across different periods at $V=300$. (a) $T=10^3$, (b) $T=10^4$, and (c) $T=10^5$

4.2 Quantitative Analysis of Demulsification Efficiency in Emulsions Under Bidirectional Triangular Pulsed Electric Fields

4.2.1 Different Electric Field Periods

Figure 9 illustrates the changes in D_r under the influence of bidirectional triangular pulsed electric fields with different periods, where V=300.

The electric field with a period $T=10^3$ reaches an inflection point in growth at $t=1.2\times10^5$, after which the change in the shape of oil droplets dominates the change in D_r. However, this change stabilizes within a specific range, indicating that the aggregation behavior of the oil droplets ends after the inflection point of growth, leading to a stabilization in the evolution of the emulsion.

The electric fields with periods $T=10^4$ and $T=10^5$ lag behind the electric field with $T=10^3$, and their D_r values simultaneously reach an inflection point in growth at $t=2.25\times10^5$. This finding suggests that the bidirectional pulsed electric fields of both periods exhibit similar demulsification efficiencies.

The results demonstrate the following: a) The demulsification efficiency of the bidirectional triangular pulsed electric field is improved at shorter period, causing a higher oil droplet aggregation rate. b) As the period is extended, the demulsification efficiency of the bidirectional triangular pulsed electric field weakens, and this reduced efficiency tends to stabilize at longer periods.

4.2.2 Different Electric Field Intensities

Figure 10. illustrates variations in D_r under the influence of bidirectional triangular pulsed electric fields with different field strengths.

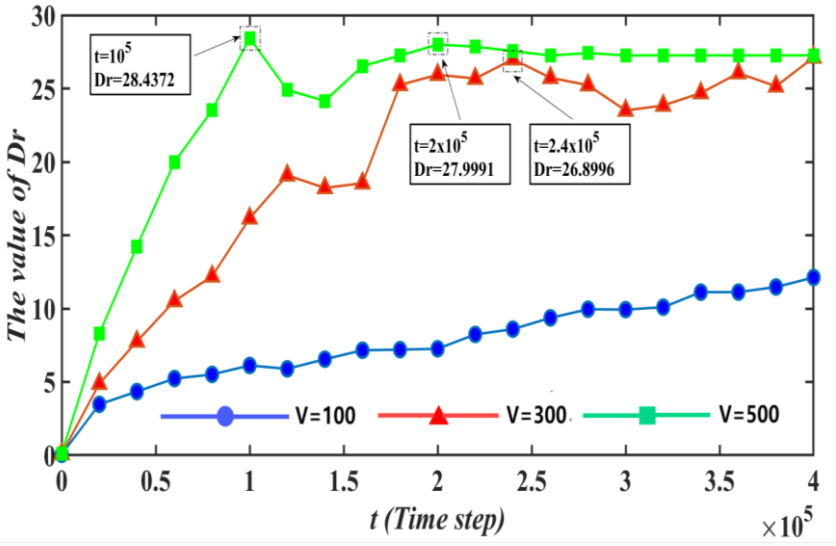

Fig. 10 Variations in D_r of emulsions under bidirectional triangular pulsed electric fields with different field strengths at $T = 10^5$. (a) $V = 100$, (b) $V = 300$, and (c) $V = 500$

At V=500, D_r reaches an inflection point in growth at $t = 10^5$. At this moment, the highest oil droplet aggregation occurs. However, D_r rapidly declines, indicating the disintegration of the oil droplets under the influence of the electric field force after aggregation. At $t = 2\times10^5$, D_r reaches another inflection point in growth, after which its value gradually stabilizes.

At V=300, D_r reaches an inflection point in growth at $t = 2.4\times10^5$. This finding suggests that the oil droplet aggregation rate at this field strength is significantly lower than that at V=500.

Compared with the first two fields, the bidirectional pulsed electric field at V=100 demonstrates a markedly lower rate of change in D_r throughout the entire time step. The lowest oil droplet aggregation rate occurs at V=100.

The findings demonstrate that high-intensity electric fields contribute to the high oil droplet aggregation rate, achieving levels significantly higher than those observed in low-intensity fields. However, oil droplets may exhibit fragmentation under the influence of high-intensity electric fields. The curve with V=500 shows stability in the later stages of oil droplet aggregation, indicating that voltages above this value will disrupt the stable state and cause the oil droplets to break apart. Therefore, the optimal voltage for oil droplet aggregation is V=500.

4.3 Conclusion from Quantitative Results

Analysis of the quantitative results presents the following:

a) The bidirectional triangular pulsed electric field achieves higher comprehensive demulsification efficiency than both DC pulsed and unidirectional triangular pulsed electric fields.

b) The use of a bidirectional triangular pulsed electric field with a small period and high intensity can achieve optimal demulsification results.

c) A bidirectional triangular pulsed electric field with high intensity can rapidly enhance demulsification efficiency. However, oil droplets may exhibit fragmentation at high intensities. Therefore, the effect of using high intensities should be considered during demulsification.

5. CONCLUSION

Through numerical simulation and quantitative analysis, this paper found that:

a) The improved bidirectional triangular pulsed electric field has good demulsification effects on dilute emulsions. Moreover, its demulsification effect is superior to that of direct current pulsed electric fields and unidirectional triangular pulsed electric fields.

b) The intensity and period of the electric field are two important parameters affecting the demulsification effect, as they directly or indirectly influence the collision probability of oil droplets.

c) Oil droplets may fragment under the action of high electric fields, but the bidirectional triangular pulsed electric field proposed in this paper does not continuously apply high intensity to the oil droplets. Therefore, the bidirectional triangular pulsed electric field can use higher electric field intensities to achieve better demulsification effects.

Additionally, there are several aspects of the bidirectional triangular pulsed electric field that require more in-depth research:

a) There exists a critical value for the electric field intensity in terms of its demulsification effect on emulsions. However, the relationship between the critical value of electric field strength and other parameters still merits investigation.

b) The pulsed electric field proposed in this paper includes a different number of waveforms within each period, and the impact of the number of waveforms on the demulsification effect still needs further investigation.

c) Extremely high electric field intensities may cause unstable turbulence in the movement of oil droplets. The current mathematical models cannot adequately simulate this situation, so improvements to the mathematical models are necessary.

ACKNOWLEDGEMENTS

We acknowledge the National Natural Science Foundation of China (Program NoS.12161058 and 12361096).

CONFLICT OF INTEREST

The author has no conflicts to disclose.

REFERENCES

Gong, H., Yu, B., Peng, Y., & Dai, F. (2019). Promoting coalescence of droplets in oil subjected to pulsed electric fields: changing and matching optimal electric field intensity and frequency for demulsification. *Journal of Dispersion Science and Technology*, *40*(9), 1236-1245. https://doi.org/:10.1080/01932691.2018.1505525

Gunstensen, A. K., Rothman, D. H., Zaleski, S., & Zanetti, G. (1991). Lattice boltzmann model of immiscible fluids. *Physical Review A*, *43*(8), 4320. https://doi.org/:10.1103/PhysRevA.43.4320

Hosseini, M., & Shahavi, M. (2012). Electrostatic enhancement of coalescence of oil droplets (in nanometer scale) in water emulsion. *Chinese Journal of Chemical Engineering*, *20*(4), 654-658. https://doi.org/:10.1016/S1004-9541(11)60231-0

Hu, J., Chen, J., Zhang, X., Xiao, J., An, S., Luan, Z., Liu, F., & Zhang, B. (2021). Dynamic demulsification of oil-in-water emulsions with electrocoalescence: Diameter distribution of oil droplets. *Separation and Purification Technology*, *254*, 117631. https://doi.org/:10.1016/j.seppur.2020.117631

Huang, X., He, L., Luo, X., & Yin, H. (2020). Droplet dynamic response in low-viscosity fluid subjected to a pulsed electric field and an alternating electric field. *AIChE Journal*, *66*(4), e16869. https://doi.org/:10.1002/aic.16869

Ichikawa, T., & Nakajima, Y. (2004). Rapid demulsification of dense oil-in-water emulsion by low external electric field.: II. Theory. *Colloids and Surfaces A: Physicochemical and Engineering Aspects*, *242*(1-3), 27-37. https://doi.org/:10.1016/j.colsurfa.2004.04.042

Latva-Kokko, M., & Rothman, D. H. (2005). Diffusion properties of gradient-based lattice Boltzmann models of immiscible fluids. *Physical Review E—Statistical,* Nonlinear*, and Soft Matter Physics*, *71*(5), 056702. https://doi.org/:10.1103/PhysRevE.71.056702

Leclaire, S., Reggio, M., & Trépanier, J. Y. (2013). Progress and investigation on lattice Boltzmann modeling of multiple immiscible fluids or components with variable density and viscosity ratios. *Journal of Computational Physics*, *246*, 318-342. https://doi.org/:10.1016/j.jcp.2013.03.039

Li, N., Pang, Y., Sun, Z., Wang, Z., Sun, X., Tang, T., Li, B., Li, W., & Zeng, H. (2023). Probing the coalescence mechanism of water droplet and Oil/Water interface in demulsification process under DC electric field. *Separation and Purification Technology*, *326*, 124798. https://doi.org/:10.1016/j.seppur.2023.124798

Liu, S., Yuan, S., & Zhang, H. (2022). Molecular dynamics simulation for the demulsification of O/W emulsion under pulsed electric field. *Molecules*, 27(8), 2559. https://doi.org/10.3390/molecules27082559

Mhatre, S., Vivacqua, V., Ghadiri, M., Abdullah, A., Al-Marri, M., Hassanpour, A., Hewakandamby, B., Azzopardi, B., & Kermani, B. (2015). Electrostatic phase separation: A review. *Chemical Engineering Research and Design*, *96*, 177-195. https://doi.org/:10.1016/j.cherd.2015.02.012

Mizoguchi, Y., & Muto, A. (2019). Demulsification of oil-in-water emulsions by application of an electric field: relationship between droplet size distribution and demulsification efficiency. *Journal of Chemical Engineering of Japan*, *52*(10), 799-804. https://doi.org/:10.1252/jcej.19we022

Mohammadian, E., Taju Ariffin, T. S., Azdarpour, A., Hamidi, H., Yusof, S., Sabet, M., & Yahya, E. (2018). Demulsification of light malaysian crude oil emulsions using an electric field method. *Industrial & Engineering Chemistry Research*, *57*(39), 13247-13256. https://doi.org/:10.1021/acs.iecr.8b02216

Peng, Y., Liu, T., Gong, H., & Zhang, X. (2016). Review of the dynamics of coalescence and demulsification by high-voltage pulsed electric fields. *International Journal of Chemical Engineering*, *2016*(1), 2492453. https://doi.org/:10.1155/2016/2492453

Qi, Z., Sun, Z., & Li, N. (2022). Effect of electric field intensity on electrophoretic migration and deformation of oil droplets in O/W emulsion under DC electric field: A molecular dynamics study. *Chemical Engineering Science, 262*, 118034. https://doi.org/10.1016/j.ces.2022.118034

Ramadhan, M. G., Khalid, N., Uemura, K., Neves, M. A., Ichikawa, S., & Nakajima, M. (2023). Efficient water removal from water-in-oil emulsions by high electric field demulsification. *Separation Science and Technology*, *58*(1), 164-174. https://doi.org/:10.1080/01496395.2022.2086882

Reis, T., & Phillips, T. N. (2007). Lattice boltzmann model for simulating immiscible two-phase flows. *Journal of Physics A: Mathematical and Theoretical*, *40*(14), 4033. https://doi.org/:10.1088/1751-8113/40/14/018

Ren, B., & Kang, Y. (2019). Aggregation of oil droplets and demulsification performance of oil-in-water emulsion in bidirectional pulsed electric field. *Separation and Purification Technology*, *211*, 958-965.

https://doi.org/:10.1016/j.seppur.2018.10.053

Tang, L., Wang, T., & Xu, Y. (2024). Research and application progress of crude oil demulsification technology. *Processes, 12*(10), 2292. https://doi.org/10.3390/pr12102292

Wang, Z., Qi, X., Zhuang, Y., Wang, Q., & Sun, X. (2023). Effect of flow field and electric field coupling on oil–water emulsion separation. *Desalination and Water Treatment*, 283, 79-96. https://doi.org/10.5004/dwt.2023.29221

Yang, C. L. (2007). Electrochemical coagulation for oily water demulsification. *Separation and Purification Technology*, *54*(3), 388-395. https://doi.org/:10.1016/j.seppur.2006.10.019

Yang, S., Sun, J., Wu, K., & Hu, C. (2021). Enhanced oil droplet aggregation and demulsification by increasing electric field in electrocoagulation. *Chemosphere*, *283*, 131123. https://doi.org/:10.1016/j.chemosphere.2021.131123

Zhang, H., Zhou, B., Zhou, X., Yang, S., Liu, S., Wang, X., Yuan, S., & Yuan, S. (2022). Molecular dynamics simulation of demulsification of O/W emulsion containing soil in direct current electric field. *Journal of Molecular Liquids*, *361*, 119618. https://doi.org/:10.1016/j.molliq.2022.119618

Zhao, Z., Kang, Y., Wu, S., & Sheng, K. (2022). Demulsification performance of oil-in-water emulsion in bidirectional pulsed electric field with starlike electrodes arrangement. *Journal of Dispersion Science and Technology*, *43*(14), 2082-2091. https://doi.org/:10.1080/01932691.2021.1915156

Zolfaghari, R., Fakhru'l-Razi, A., Abdullah, L. C., Elnashaie, S. S., & Pendashteh, A. (2016). Demulsification techniques of water-in-oil and oil-in-water emulsions in petroleum industry. *Separation and Purification Technology*, *170*, 377-407. https://doi.org/:10.1016/j.seppur.2016.06.026